ISSN 1063-7737, Astronomy Letters, 2012, Vol. 38, No. 7, pp. 411–427. © Pleiades Publishing, Inc., 2012.
Original Russian Text © V.V. Vityazev, A.S. Tsvetkov, 2012, published in Pis'ma v Astronomicheskiĭ Zhurnal, 2012, Vol. 38, No. 7, pp. 467–485.

Kinematics of Stars in the Northern and Southern Galactic Hemispheres

V. V. Vityazev* **and A. S. Tsvetkov****

St. Petersburg State University, Bibliotechnaya pl. 2, St. Petersburg, 198504 Russia

Received November 12, 2011

Abstract—We use vector spherical harmonics for a kinematic analysis of the proper motions of stars from the Hipparcos, Tycho-2, and UCAC3 catalogues in the northern and southern Galactic hemispheres. We have found that the statistically reliable values of the Ogorodnikov–Milne model parameters M_{32}^{+} and M_{32}^{-} have different signs in different hemispheres. This is a consequence of the Galaxy's rotational retardation with distance from the principal Galactic plane. Based on various samples of stars from the above catalogues, we have obtained the following estimate for the magnitude of the vertical gradient of Galactic rotation velocity in the solar neighborhoods: $(20.1 \pm 2.9) < |\partial V_{\odot}/\partial z| < (49.2 \pm 0.8)$ km s^{-1} kpc^{-1}. Another result that is revealed by our analysis of the parameters M_{13}^{-} and M_{13}^{+} in different Galactic hemispheres is that the vertical gradient of expansion velocity for the stellar system $\partial V_R/\partial z$ is positive in the northern hemisphere and negative in the southern one. This suggests that the expansion velocity V_R increases with distance from the Galactic plane. We show that both these gradients give rise to an apparent acceleration of the solar motion along the x and y axes of the rectangular Galactic coordinate system. Our analysis of the parameters M_{21}^{-} and M_{12}^{+} shows no significant differences in both hemispheres and has allowed us to determine the Oort parameters, to estimate the Galactic rotation velocity and period in the solar neighborhood, and to calculate the ratio of the epicyclic frequency to the angular velocity of Galactic rotation in the solar neighborhood. The derived diagonal elements of the velocity field deformation tensor suggest that the orientation of the rectangular Galactic coordinate system in space must be determined by taking into account not only the geometrical factors but also the dynamical ones. All these results agree well with these quantities estimated over the entire sphere by various authors.

DOI: 10.1134/S1063773712060060

Keywords: *all-sky star catalogues, stellar proper motions, Galactic kinematics, vector spherical harmonics.*

INTRODUCTION

Investigation of the stellar motions in circumsolar space is an important tool for studying the Galaxy. It is based on an analysis of the stellar proper motions and radial velocities within various kinematic models. The success of a kinematic analysis of the velocity field is largely determined by the quality and quantity of observational data. The last two decades have been marked by rapid progress in astrometry, in particular, in producing highly accurate all-sky star catalogues of stellar positions and proper motions. In 1997 the Hipparcos catalogue containing more than 100 thousand stars was published (Perriman et al. 1997); the Tycho-2 catalogue containing highly accurate proper motions for 2.5 million stars was published three years after (Hog et al. 2000). Subsequently, the USNO-B catalogue (Monet 2003) with more than 1 billion objects appeared, but the accuracy of the stellar positions in this catalogue is low and there are proper motions (of mediocre quality) only for a third of the stars. In 2009 the work on the UCAC3 catalogue had been finished at the US Naval Observatory (Zacharias et al. 2009). The catalogue contains the positions, accurate proper motions, and photometric data for 100 million stars to 17^m. Near-infrared photometry from the 2MASS project (Skrutskie et al. 2006) is also provided for most of the stars. Despite the defects in constructing the catalogue in the northern hemisphere (Roeser et al. 2010), it is a very rich material for studying the Galactic kinematics.

The appearance of these all-sky star catalogs and the prospects for measuring highly accurate parallaxes, proper motions, and radial velocities for hundreds of millions of stars planned in the GAIA project (Coryn and Bailer-Jones 2004) are a stimulus for developing new methods of kinematic analysis of stars. The papers by Vityazev and Shuksto (2004) and Vityazev and Tsvetkov (2009, 2011), which are de-

*E-mail: vityazev@list.ru
**E-mail: a.s.tsvetkov@inbox.ru

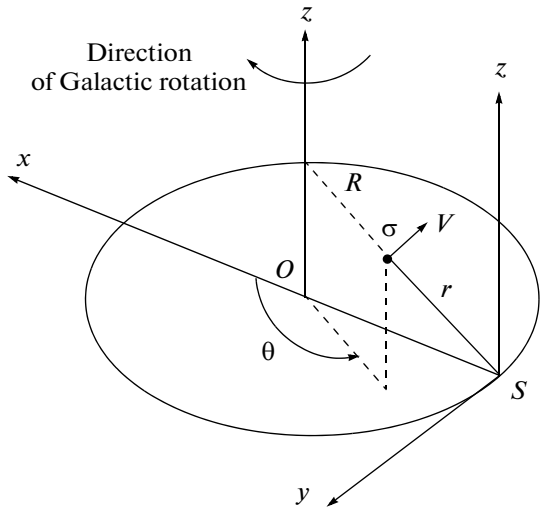

Rectangular Galactic coordinate system (x, y, z) and Galactic cylindrical coordinate system (R, θ, z). O is the Galactic center, σ is the position of a star, S is the position of the Sun.

voted to the application of vector spherical harmonics (VSHs) to stellar kinematics problems, meet this requirement. Using VSHs allows all systematic components in the stellar velocity field to be revealed without attaching to a specific physical model. Comparison of the decomposition coefficients for a specific kinematic model with observational data can reveal the systematic components that are not described by this model. The VSH method was also used by other authors (see, e.g., Makarov and Murphy 2007; Bobylev et al. 2011).

Note that the VSH method was developed for astrometric catalogues in which the stars are distributed uniformly over the entire celestial sphere. Previously (Vityazev and Tsvetkov 2011), we adapted the VSH method to a kinematic analysis of the proper motions for stars from the Tycho-2 Spectral Types catalogue located only in the southern equatorial hemisphere, because this catalogue contains information about the two-dimensional spectral classification of stars mostly for stars in the southern hemisphere of the equatorial coordinate system.

The goal of this paper is to use VSHs to study the stellar kinematics based on stars distributed not over the entire sphere, as it was previously, but concentrated in the northern and southern Galactic hemispheres. The formulation of this problem is justified from a physical viewpoint, because the possibly existing kinematic differences in both hemispheres may not be revealed by a global analysis, compensating one another partially or completely. For this purpose, we constructed the systems of VSHs with the properties of completeness and orthogonality in the northern and southern Galactic hemispheres. Subsequently, we derived the formulas that allowed the parameters of the Ogorodnikov–Milne model to be estimated via the derived coefficients of the decomposition of proper motions into a system of zonal vector spherical harmonics. We showed that our approach allows the parameters to be estimated at least by the main and alternative methods. Comparison of the main and alternative solutions allows the consistency of the standard kinematic model with the observational data to be tested. The developed method was tested on the basis of numerical experiments and then applied to investigate various samples of stars from the Hipparcos, Tycho-2, and UCAC3 catalogues. Analysis of the calculations showed that some of the Ogorodnikov–Milne model parameters turned out to be significantly different in different hemispheres, while other parameters, on the contrary, underwent no significant changes when passing from one hemisphere to the other.

CLASSICAL KINEMATIC MODELS

The equations of the Ogorodnikov–Milne model (Ogorodnikov 1965; du Mont 1977) are commonly used to investigate the kinematics of stars. In this model, the stellar velocity field is represented by the linear expression

$$\mathbf{V} = \mathbf{V}_0 + M\mathbf{r}, \tag{1}$$

where $\mathbf{V}$ is the total velocity of the star, $\mathbf{V}_0$ is the observer's centroid velocity, M is the displacement matrix, and $\mathbf{r}$ is the heliocentric radius vector of the star. Let us introduce a rectangular Galactic system of coordinates x, y, z whose origin coincides with the Sun's position, the x axis is directed toward the Galactic center, the y axis is in the direction of Galactic rotation, and the z axis is perpendicular to the Galactic plane (see the figure). Consider the matrix of transformation from the unit vectors $\mathbf{e}_x$, $\mathbf{e}_y$, $\mathbf{e}_z$ of the rectangular Galactic coordinate system to the unit vectors $\mathbf{e}_l$, $\mathbf{e}_b$, $\mathbf{e}_r$ pointing, respectively, in the direction of increasing Galactic longitudes and latitudes and along the line of sight:

$$A(l,b) = \begin{bmatrix} -\sin l & \cos l & 0 \\ -\cos l \sin b & -\sin l \sin b & \cos b \\ \cos l \cos b & \sin l \cos b & \sin b \end{bmatrix}. \tag{2}$$

Projecting the vector $\mathbf{V}$ onto the unit vectors $\mathbf{e}_l$, $\mathbf{e}_b$, $\mathbf{e}_r$, we will obtain

$$\begin{bmatrix} \mathcal{K}\mu_l \cos b \\ \mathcal{K}\mu_b \\ V/r \end{bmatrix} = A(l,b) \begin{bmatrix} U/r \\ V/r \\ W/r \end{bmatrix} \tag{3}$$

$$+ A(l,b)M \begin{bmatrix} \cos b \cos l \\ \cos b \sin l \\ \sin b \end{bmatrix}.$$

In the Ogorodnikov–Milne method, the displacement matrix is usually represented as

$$M = M^+ + M^-, \tag{4}$$

where M^+ is the symmetric local velocity field deformation matrix

$$M^+ = \begin{bmatrix} M_{11}^+ & M_{12}^+ & M_{13}^+ \\ M_{21}^+ & M_{22}^+ & M_{23}^+ \\ M_{31}^+ & M_{32}^+ & M_{33}^+ \end{bmatrix}, \tag{5}$$

M^- is the antisymmetric local rotation matrix

$$M^- = \begin{bmatrix} M_{11}^- & M_{12}^- & M_{13}^- \\ M_{21}^- & M_{22}^- & M_{23}^- \\ M_{31}^- & M_{32}^- & M_{33}^- \end{bmatrix} \tag{6}$$

$$= \begin{bmatrix} 0 & -\Omega_3 & \Omega_2 \\ \Omega_3 & 0 & -\Omega_1 \\ -\Omega_2 & \Omega_1 & 0 \end{bmatrix}.$$

In addition, the vector $\mathbf{V}_0$ is usually interpreted as the effect of solar motion relative to the chosen centroid of stars with components U, V, W:

$$\mathbf{V}_0 = -U\mathbf{e}_x - V\mathbf{e}_y - W\mathbf{e}_z. \tag{7}$$

Thus, the Ogorodnikov–Milne model contains 12 parameters: U, V, W are the components of the solar motion vector $\mathbf{V}_0$ relative to the centroid of stars; Ω_1, Ω_2, Ω_3 are the components of the rigid-body rotation vector $\mathbf{\Omega}$ of the centroid of stars; M_{11}^+, M_{22}^+, M_{33}^+ are the parameters of the tensor $\mathbf{M}^+$ describing the velocity field contraction–expansion along the principal axes of the coordinate system; $M_{12}^+ = M_{21}^+$, $M_{13}^+ = M_{31}^+$, $M_{23}^+ = M_{32}^+$ are the parameters of the tensor M^+ describing the velocity field deformation in the principal plane and the two planes perpendicular to it.

Below, we give the Ogorodnikov–Milne model equations in the Galactic coordinate system in explicit form:

$$\begin{aligned} \mathcal{K}\mu_l \cos b = {} & U/r \sin l - V/r \cos l \\ & - \Omega_1 \sin b \cos l - \Omega_2 \sin b \sin l + \Omega_3 \cos b \\ & - M_{13}^+ \sin b \sin l + M_{23}^+ \sin b \cos l \\ & + M_{12}^+ \cos b \cos 2l - \frac{1}{2} M_{11}^+ \cos b \sin 2l \\ & + \frac{1}{2} M_{22}^+ \cos b \sin 2l, \end{aligned} \tag{8}$$

$$\begin{aligned} \mathcal{K}\mu_b = {} & U/r \cos l \sin b + V/r \sin l \sin b \\ & - W/r \cos b + \Omega_1 \sin l - \Omega_2 \cos l \\ & - \frac{1}{2} M_{12}^+ \sin 2b \sin 2l + M_{13}^+ \cos 2b \cos l \\ & + M_{23}^+ \cos 2b \sin l - \frac{1}{2} M_{11}^+ \sin 2b \cos^2 l \\ & - \frac{1}{2} M_{22}^+ \sin 2b \sin^2 l + \frac{1}{2} M_{33}^+ \sin 2b, \end{aligned} \tag{9}$$

$$\begin{aligned} V_r/r = {} & -U/r \cos l \cos b - V/r \sin l \cos b \\ & - W/r \sin b + M_{13}^+ \sin 2b \cos l + M_{23}^+ \sin 2b \sin l \\ & + M_{12}^+ \cos^2 b \sin 2l + M_{11}^+ \cos^2 b \cos^2 l \\ & + M_{22}^+ \cos^2 b \sin^2 l + M_{33}^+ \sin^2 b. \end{aligned} \tag{10}$$

Since there is a linear relation between the coefficients M_{11}^+, M_{22}^+, M_{33}^+ in Eqs. (8) and (9), the substitutions $M_{11}^* = M_{11}^+ - M_{22}^+$ and $M_{33}^* = M_{33}^+ - M_{22}^+$ are usually introduced and the parameter M_{22}^+ is omitted when the stellar proper motions are analyzed.

Let us relate the rotation and deformation tensor elements with the velocity field components V_R, V_θ, and V_z in the Galactocentric cylindrical coordinate system (R, θ, z), where R is the radius vector, θ is the azimuthal angle measured from the x axis counterclockwise, and z is the distance from the Galactic plane (see the figure). For the off-diagonal parameters of the matrices M^+ and M^- of the Ogorodnikov–Milne model in this coordinate system, we have (Miyamoto et al. 1993)

$$\begin{aligned} 2M_{12}^+ &= \frac{\partial V_\theta}{\partial R} - \frac{V_\theta}{R} + \frac{1}{R}\frac{\partial V_R}{\partial \theta}; \\ 2M_{21}^- &= \frac{\partial V_\theta}{\partial R} + \frac{V_\theta}{R} - \frac{1}{R}\frac{\partial V_R}{\partial \theta}; \end{aligned} \tag{11}$$

$$\begin{aligned} 2M_{13}^+ &= -\frac{\partial V_R}{\partial z} - \frac{\partial V_z}{\partial R}; \\ 2M_{13}^- &= -\frac{\partial V_R}{\partial z} + \frac{\partial V_z}{\partial R}; \end{aligned} \tag{12}$$

$$\begin{aligned} 2M_{32}^+ &= -\frac{1}{R}\frac{\partial V_z}{\partial \theta} - \frac{\partial V_\theta}{\partial z}; \\ 2M_{32}^- &= -\frac{1}{R}\frac{\partial V_z}{\partial \theta} + \frac{\partial V_\theta}{\partial z}. \end{aligned} \tag{13}$$

In turn, the diagonal elements of the matrices M^+ are represented as

$$\begin{aligned} M_{11}^+ = \frac{\partial V_z}{\partial R}; \quad M_{22}^+ = \frac{V_R}{R} + \frac{1}{R}\frac{\partial V_\theta}{\partial \theta}; \\ M_{33}^+ = -\frac{\partial V_z}{\partial z}. \end{aligned} \tag{14}$$

The velocity field is usually analyzed using the solution of the main kinematic equations (8)–(10) for the Ogorodnikov–Milne model parameters in the local coordinate system comoving with the Sun around the Galactic center. Passing to the Galactocentric cylindrical coordinate system helps obtain information referring to the Galaxy as a whole.

Sometimes, the three-dimensional Ogorodnikov–Milne model is replaced with a simplified one, in which in addition to the solar motion components, only the quantities $A = M_{12}^{+}$, the velocity field deformation in the Galactic plane, and $B = \Omega_3$, the rotation vector of the entire stellar system also in the Galactic plane, are determined from the equations for proper motions based on the hypothesis of plane Galactic rotation. These quantities are called the Oort parameters, while the model itself is called the Oort–Lindblad model (Ogorodnikov 1965). The difference $\omega = A - B$ gives the angular velocity of Galactic rotation in the solar neighborhood. Second-order equations, for example, the generalized Oort model, which can be found in Ogorodnikov (1965), Edmondson (1937), and Branham (2002), are occasionally considered.

All these models have two shortcomings. First, the question of whether the model is consistent with the observations, i.e., whether it is complete, and whether it imposes nonexisting properties on the actual stellar velocity field, always remains. This problem has already been considered previously (see Vityazev and Shuksto 2004; Vityazev and Tsvetkov 2009). However, there is a second problem that has eluded the researchers. All models implicitly assume that the stellar velocity field in the solar neighborhood is isotropic in the sense that the components of the rotation–deformation tensor (4) are identical for all directions on the celestial sphere. Samples of stars as homogeneous as possible and covering the celestial sphere as uniformly as possible were commonly used to determine the model parameters. As we will see, this approach could not reveal the existing asymmetry in the stellar proper motions.

MATHEMATICAL METHODS OF KINEMATIC ANALYSIS

The standard method of determining the velocity field parameters consists in writing conditional equations for the chosen model, for example, (8)–(10), and solving them by the least-squares technique (below referred to as the LST), which gives the most probable values of the sought-for parameters and their rms errors. The separate or combined solutions of the equations are performed. Different weights can also be assigned to the equations. This method is widely used in practice. However, as has already been said, its shortcoming is that we impose a model chosen in advance on the proper motions. There can be systematic components that are not described by the model in the proper motions. Here, two situations are possible. The LST "will not notice" them and the information contained in them will go into an increase in the rms errors. The second situation is worse: the unknown systematic components can penetrate into the model parameters, distorting them. The situation where the effect described by the model is absent in the velocity field, while the unknown component, nevertheless, will give rise to a significant value of one or more model parameters is even possible. As a result, we will obtain estimates of the parameters for those phenomena that are actually absent in the observational data. Of course, the LST can be applied to study the velocity field not only on the entire sphere but also in its separate parts, in particular, on a hemisphere. In practice, however, this leads to significant correlations between the parameters (up to 0.9), which casts doubt on the results obtained. As we showed previously (Vityazev and Tsvetkov 2011), this shortcoming can be removed via zonal vector spherical harmonics.

Brosche (1966) was the first to suggest using (scalar) spherical harmonics to analyze the systematic differences of the stellar positions and proper motions. The first attempt to apply spherical harmonics to a kinematic analysis of the proper motions was made by Vityazev and Tsvetkov (1989). Since the stellar proper motions are vectorial in nature, it is natural to use **vector spherical harmonics** (below referred to as VSHs) to analyze the stellar proper motions. The method of constructing a system of these harmonics was described by Arfken (1970). VSHs were first applied to analyze the local kinematics of stars by Vityazev and Shuksto (2004). The VSH apparatus and its use in a general analysis of the stellar proper motions and radial velocities were described previously (Vityazev and Tsvetkov 2009). In these papers, VSHs revealed strong systematic components that were not described by the standard models.

However, although VSHs are complete on the sphere and reveal all systematic components in the stellar proper motions, they cannot be applied in the cases where we wish to investigate the kinematics of only a part of the celestial sphere. To solve problems of this kind, we suggest using a specially constructed set of vector spherical harmonics.

Zonal Vector Spherical Harmonics

The zonal vector spherical harmonics (below referred to as ZVSHs) are determined for some Galactic latitude (declination) zone and can be used in

the northern or southern hemispheres of the celestial sphere. They are obtained by slightly modifying the ordinary VSHs determined on the entire sphere.

Let we have a catalogue whose data belong to the following region of the celestial sphere:

$$Z = \begin{cases} 0 \le l \le 2\pi, \\ b_{\min} \le b \le b_{\max}. \end{cases} \quad (15)$$

Let us introduce the transformation

$$\hat{b} = \arcsin(P \sin b + Q), \quad (16)$$

that at

$$P = \frac{2}{s_2 - s_1}, \quad Q = -\frac{s_2 + s_1}{s_2 - s_1}, \quad (17)$$

$$s_1 = \sin b_{\min}, \qquad s_2 = \sin b_{\max}, \quad (18)$$

transforms the entire sphere into region Z.

Consider a system of mutually orthogonal unit vectors $\mathbf{e}_l$ and $\mathbf{e}_b$ in the directions of change in longitude and latitude, respectively, in a tangent plane to the sphere. Let us introduce the toroidal, $\mathbf{T}_{nks}$, and spheroidal, $\mathbf{S}_{nks}$, VSHs via the relations

$$\mathbf{T}_{nks} = \frac{1}{\sqrt{n(n+1)}} \quad (19)$$
$$\times \left(\frac{\partial K_{nks}(l,\hat{b})}{\partial \hat{b}} \mathbf{e}_l - \frac{1}{\cos b} \frac{\partial K_{nks}(l,\hat{b})}{\partial l} \mathbf{e}_b \right),$$

$$\mathbf{S}_{nks} = \frac{1}{\sqrt{n(n+1)}} \quad (20)$$
$$\times \left(\frac{1}{\cos b} \frac{\partial K_{nks}(l,\hat{b})}{\partial l} \mathbf{e}_l + \frac{\partial K_{nks}(l,\hat{b})}{\partial \hat{b}} \mathbf{e}_b \right).$$

For brevity, we will denote the components at the unit vector $\mathbf{e}_l$ by T^l_{nks} and S^l_{nks} and at the unit vector $\mathbf{e}_b$ by T^b_{nks} and S^b_{nks}, respectively:

$$\mathbf{T}_{nks} = T^l_{nks}\mathbf{e}_l + T^b_{nks}\mathbf{e}_b, \quad (21)$$

$$\mathbf{S}_{nks} = S^l_{nks}\mathbf{e}_l + S^b_{nks}\mathbf{e}_b. \quad (22)$$

In Eqs. (19) and (20), $K_{nks}(l,\hat{b})$ denote the scalar spherical harmonics:

$$K_{nks}(l,b) \quad (23)$$
$$= R_{nk} \begin{cases} P_{n,0}(\hat{b}), & k = 0, \quad s = 1, \\ P_{nk}(\hat{b}) \sin kl, & k \ne 0, \quad s = 0, \\ P_{nk}(\hat{b}) \cos kl, & k \ne 0, \quad s = 1, \end{cases}$$

where $P_{nk}(\hat{b})$ are the Legendre polynomials at $k = 0$ and the associated Legendre polynomials at $k > 0$.

It is easy to show that if the normalization factor in Eq. (23) is specified by the expression

$$R_{nk} = \sqrt{P\frac{2n+1}{4\pi}} \begin{cases} \sqrt{\frac{2(n-k)!}{(n+k)!}}, & k > 0, \\ 1, & k = 0, \end{cases} \quad (24)$$

then our VSHs will satisfy the relations

$$\iint\limits_Z (\mathbf{T}_i \cdot \mathbf{T}_j)\, d\omega = \iint\limits_Z (\mathbf{S}_i \cdot \mathbf{S}_j)\, d\omega \quad (25)$$
$$= \begin{cases} 0, & i \ne j, \\ 1, & i = j, \end{cases}$$

$$\iint\limits_Z (\mathbf{S}_i \cdot \mathbf{T}_j)\, d\omega = 0, \ \ \forall i, j. \quad (26)$$

In other words, $\mathbf{T}_{nkp}(l,\hat{b})$ and $\mathbf{S}_{nkp}(l,\hat{b})$ form an orthonormal system of functions on set Z. Note also that a linear numbering of the functions $\mathbf{T}_{nks}$ and $\mathbf{S}_{nks}$ by one index j, where

$$j = n^2 + 2k + s - 1 \quad (27)$$

is often introduced.

Explicit formulas for calculating the Legendre polynomials $P_{nk}(b)$ and the components T^l_{nks}, T^b_{nks}, S^l_{nks}, and S^b_{nks} are given in our previous papers (Vityazev and Tsvetkov 2009, 2011).

DECOMPOSITION OF THE OGORODNIKOV–MILNE MODEL EQUATIONS INTO A SYSTEM OF ZVSHs

As in the case of VSHs on the entire sphere, for the system of ZVSHs we can obtain a theoretical decomposition of Eqs. (8) and (9). Here, we will restrict our analysis only to two zones: the northern ($b > 0$) and southern ($b \le 0$) Galactic hemispheres. The initial decomposition coefficients are presented in Table 1 in the form of formulas explaining the physical meaning of the toroidal and spheroidal coefficients within the Ogorodnikov–Milne model.

Since the ZVSHs are orthogonal in the specified part of the celestial sphere, in contrast to the direct determination of model parameters by the LST, the correlations between the coefficients to be determined will be close to zero. A very important circumstance should be noted. Whereas the VSH decomposition of Eqs. (8) and (9) is finite (Vityazev and Tsvetkov 2009), the ZVSH decomposition of the same equations is infinite. Each parameter (or their linear combination) produces a whole series of decreasing coefficients. This feature of the decomposition opens the remarkable possibility of determining the model parameters from several sets of coefficients.

Table 1. Theoretical values of the initial ZVSH decomposition coefficients T_j and S_j

j	n	k	l	T_j	S_j
1	1	0	1	$+1.949\Omega_3$	$-1.949W/\langle r\rangle \pm 0.873M_X$
2	1	1	0	$\mp 0.768U/\langle r\rangle + 1.791\Omega_2 - 0.256M_{13}^+$	$-1.791V/\langle r\rangle \mp 0.768\Omega_1 \pm 1.279M_{23}^+$
3	1	1	1	$\pm 0.768V/\langle r\rangle + 1.791\Omega_1 + 0.256M_{23}^+$	$-1.791U/\langle r\rangle \mp 0.768\Omega_2 \pm 1.279M_{13}^+$
4	2	0	1	$\mp 0.453\Omega_3$	$\pm 0.453W + 0.274M_X$
5	2	1	0	$+0.332U/\langle r\rangle \mp 0.332\Omega_2 \pm 0.332M_{13}^+$	$\pm 0.332V/\langle r\rangle + 0.332\Omega_1 + 0.728M_{23}^+$
6	2	1	1	$-0.332V/\langle r\rangle \mp 0.332\Omega_1 \mp 0.332M_{23}^+$	$\pm 0.332U/\langle r\rangle - 0.332\Omega_2 + 0.728M_{13}^+$
7	2	2	0	$\pm 0.216M_{11}^*$	$+1.338M_{12}^+$
8	2	2	1	$\mp 0.433M_{12}^+$	$+0.669M_{11}^*$
9	3	0	1	$+0.270\Omega_3$	$-0.270W/\langle r\rangle \mp 0.017M_X$
10	3	1	0	$\mp 0.199U/\langle r\rangle + 0.199\Omega_2 - 0.199M_{13}^+$	$-0.199V/\langle r\rangle \mp 0.199\Omega_1 \mp 0.199M_{23}^+$
11	3	1	1	$\pm 0.199V/\langle r\rangle + 0.199\Omega_1 + 0.199M_{23}^+$	$-0.199U/\langle r\rangle \pm 0.199\Omega_2 \mp 0.199M_{13}^+$
12	3	2	0	$-0.109M_{11}^*$	$\mp 0.463M_{12}^+$
13	3	2	1	$+0.219M_{12}^+$	$\mp 0.231M_{11}^*$
14	3	3	0	0	0
15	3	3	1	0	0

Note. The upper and lower signs correspond to the northern and southern hemispheres, respectively; if there is one sign, then the signs of the coefficients are identical for the northern and southern hemispheres. The following notation is used in the table: $M_{11}^* = M_{11}^+ - M_{22}^+$, $M_X = M_{33}^+ - \frac{1}{2}(M_{11}^+ + M_{22}^+)$. The units of measurement are km s^{-1} kpc^{-1}.

Comparison of the values obtained will allow us to judge whether the model is consistent (in the case of close values) with the observations. In practice, we used only two sets of coefficients via which we obtained two sets of Ogorodnikov–Milne model parameters. We called these solutions the main and alternative ones.

The main and alternative solutions for the proper motions can be represented as

$$\begin{bmatrix} U/\langle r\rangle \\ V/\langle r\rangle \\ W/\langle r\rangle \\ \Omega_1 \\ \Omega_2 \\ \Omega_3 \\ M_{13}^+ \\ M_{23}^+ \\ M_{12}^+ \\ M_{11}^* \\ M_{33}^* \end{bmatrix} = \mathbf{A} \begin{bmatrix} s_{101} \\ s_{110} \\ s_{111} \\ s_{201} \\ s_{210} \\ s_{211} \\ s_{220} \\ s_{221} \\ t_{101} \\ t_{110} \\ t_{111} \end{bmatrix}, \qquad (28)$$

$$\begin{bmatrix} U/\langle r\rangle \\ V/\langle r\rangle \\ W/\langle r\rangle \\ \Omega_1 \\ \Omega_2 \\ \Omega_3 \\ M_{13}^+ \\ M_{23}^+ \\ M_{12}^+ \\ M_{11}^* \\ M_{33}^* \end{bmatrix} = \mathbf{B} \begin{bmatrix} s_{101} \\ s_{110} \\ s_{111} \\ s_{301} \\ t_{201} \\ t_{110} \\ t_{111} \\ t_{210} \\ t_{211} \\ t_{220} \\ t_{221} \end{bmatrix}.$$

Numerical values for the elements of the matrices **A** and **B** for the northern and southern hemispheres are given in Tables 2 and 3.

It should be kept in mind that the solar motion components enter into Eqs. (28) with the factor $1/\langle r\rangle$. This means that when using ZVSHs, either the effects of solar motion should be eliminated or it makes sense to perform the solution only for stars at approximately the same heliocentric distance; in this case, we will be able to determine the solar motion parameters only to within the factor $1/\langle r\rangle$.

Table 2. Matrix **A** for calculating the main solution (28)

0	0	−0.54	0	0	±1.10	0	0	0	±0.44	0
0	−0.54	0	0	±1.10	0	0	0	0	0	∓0.44
−0.29	0	0	±0.94	0	0	0	0	0	0	0
0	±0.21	0	0	−0.64	0	0	0	0	0	0.77
0	0	∓0.21	0	0	0.64	0	0	0	0.77	0
0	0	0	0	0	0	0	0	0.51	0	0
0	0	±0.15	0	0	1.16	0	0	0	0.15	0
0	±0.15	0	0	1.16	0	0	0	0	0	−0.15
0	0	0	0	0	0	0.75	0	0	0	0
0	0	0	0	0	0	0	1.49	0	0	0
±0.49	0	0	2.10	0	0	0	0.75	0	0	0

Note. The upper and lower signs correspond to the northern and southern hemispheres, respectively; if there is one sign, then the signs of the coefficient are identical for the northern and southern hemispheres.

Table 3. Matrix **B** for calculating the alternative solution (28)

0	0	−0.42	0	0	±0.56	0	2.04	0	0	0
0	−0.42	0	0	0	0	∓0.56	0	−2.04	0	0
−0.06	0	0	−3.25	0	0	0	0	0	0	0
0	±0.14	0	0	0	0	0.84	0	±1.18	0	0
0	0	∓0.14	0	0	0.84	0	±1.18	0	0	0
0	0	0	0	∓2.21	0	0	0	0	0	0
0	0	±0.28	0	0	0.28	0	±2.15	0	0	0
0	±0.28	0	0	0	0	−0.28	0	∓2.15	0	0
0	0	0	0	0	0	0	0	0	0	∓2.31
0	0	0	0	0	0	0	0	0	±4.63	0
±1.00	0	0	∓7.25	0	0	0	0	0	±2.32	0

Note. The upper and lower signs correspond to the northern and southern hemispheres, respectively; if there is one sign, then the signs of the coefficient are identical for the northern and southern hemispheres.

Thus, using ZVSHs allow us: (1) to obtain the solution on a hemisphere, avoiding strong correlations between the parameters to be determined; (2) to use the derived decomposition coefficients to calculate the parameters of any kinematic model; (3) to test the model for consistency with the observations by comparing the main and alternative solutions; (4) to find the decomposition coefficients that are not predicted by the chosen model.

APPLICATION OF ZVSHs IN PRACTICE

The volume of processed data from each all-sky astrometric catalogue (especially UCAC3) is very large. Indeed, the density of 14^m–15^m stars in this catalogue is about 100 stars pere square degree in

polar regions and exceeds 1000 stars per square degree for latitudes $|b| < 20°$. There is only a small region with an anomalously low density along the celestial equator. This is probably due to the technical peculiarities of constructing the catalog. As a result, a direct determination of the VSH decomposition coefficients runs into certain technical difficulties. These difficulties can be overcome by data pre-pixelization on the sphere. As applied to our problem, the pixelization scheme should satisfy the requirement that the pixel centers are equidistant in both latitude and longitude. Two schemes satisfy this requirement. One of them is HEALPix (Gorski 2005); the other is the so-called Equidistant Cylindrical Projection (ECP). The pixelization algorithms were discussed in detail previously (Vityazev and Tsvetkov 2009). In this paper, we dwelt on ECP, in which the stellar proper motions are averaged over spherical trapeziums obtained by a uniform division of the equator and the latitude circle into M and N parts, respectively.

For each field, we calculated the average proper motions $\langle \mathcal{K}\mu_l \cos b\rangle$ and $\langle \mathcal{K}\mu_b\rangle$ of the stars that fell into this field. We chose $M = 180$ and $N = 90$ for the UCAC3 catalogue, which allowed the values of very high harmonics to be determined, but, for our purposes, we restricted ourselves to the determination of 35 toroidal and 35 spheroidal coefficients. They were determined by solving the equations

$$\mathcal{K}\mu_l \cos b = \sum_{nkp} t_{nkp}\mathbf{T}^l_{nkp}(l,\hat{b}) + \sum_{nkp} s_{nkp}\mathbf{S}^l_{nkp}(l,\hat{b}), \quad (29)$$

$$\mathcal{K}\mu_b = \sum_{nkp} t_{nkp}\mathbf{T}^b_{nkp}(l,\hat{\delta}) + \sum_{nkp} s_{nkp}\mathbf{S}^b_{nkp}(l,\hat{b}) \quad (30)$$

by the LST with the assignment of a weight to each field equal to the number of stars that fell into it. The fields into which fewer than three stars fell were excluded. Once the coefficients t_{nkp} and s_{nkp} have been determined, we reconstructed the Ogorodnikov–Milne model parameters from Eqs. (28) and compared the main and alternative solutions between themselves.

Before analyzing the actual proper motions, we performed numerous tests with artificial proper motions to determine whether the VSH method was stable against random errors and whether the method could reveal various systematic components. All tests showed a high reliability of the results obtained, their stability against noise, and the coincidence of the main and alternative solutions in the model cases. As applied to a kinematic analysis of the stellar proper motions for the southern equatorial hemisphere, these tests were described previously (Vityazev and Tsvetkov 2011).

ANALYSIS

We applied ZVSHs to investigate the proper motions of stars in the northern and southern Galactic hemispheres using data from the Hipparcos, Tycho-2, and UCAC3 catalogues. The following samples were produced: (1) HIP. R, 250–500—red giants from the Hipparcos catalogue in the range of distances from 250 to 500 pc (7280 stars); (2) Tycho-2 R, 10^m–12^m—red giants from the Tycho-2 catalogue in the range of magnitudes 10^m–12^m (170 560 stars); (3) UCAC3, 12^m (1 662 874 stars); (4) UCAC3, 13^m (3 117 661 stars); (5) UCAC3, 14^m (6 779 891 stars); (6) UCAC3, 15^m (13 257 192 stars); (7) UCAC3, 16^m (16 200 463 stars).

The ZVSH decomposition coefficients were calculated for all groups of stars from these catalogues. As an example, here we present only the results obtained for the UCAC3 15^m stars. The initial coefficients are listed in Table 4. The main and alternative solutions for several groups of 12^m–16^m stars from the same catalogue are given in Tables 5 and 6. The solution obtained over the entire sphere for the UCAC3 stars is presented in Table 7. Below we comment our results in accordance with the physical effects that are described by various Ogorodnikov–Milne model parameters. Let us first describe the parameters that turned out to be different in the northern and southern Galactic hemispheres and then dwell on the results that turned out to be essentially identical in both hemispheres.

Analysis of the Parameters M^-_{32} and M^+_{32}. The Vertical Gradient of the Galaxy's Rotation Velocity

The most striking result that we obtained when analyzing the velocity field in different hemispheres is that the statistically reliable values of M^+_{32} and M^-_{32} have different signs in different hemispheres. For example, the mean values of $\Omega_1 = M^-_{32}$ obtained from the UCAC3 12^m–16^m stars in the northern and southern hemispheres are $+21.0 \pm 0.3$ and -25.0 ± 0.3 km s^{-1} kpc^{-1}, respectively. As can be seen from Tables 5 and 6, the reality of this parameter is confirmed by excellent agreement between the main and alternative solutions, where an almost complete coincidence is observed, within the error limits of this parameter. When the kinematic parameters are traditionally determined by the LST from data over the

Table 4. Toroidal, T_j, and spheroidal, S_j, VSH decomposition coefficients for the UCAC3 15^m stars

j	n	k	l	Northern hemisphere		Southern hemisphere	
				T_j	S_j	T_j	S_j
1	1	0	1	-29.30 ± 0.63	-3.71 ± 0.63	-37.75 ± 0.64	-8.57 ± 0.64
2	1	1	0	-33.36 ± 0.67	-39.10 ± 0.67	6.70 ± 0.68	-52.54 ± 0.68
3	1	1	1	41.50 ± 0.67	-29.45 ± 0.67	-34.26 ± 0.66	-9.61 ± 0.66
4	2	0	1	14.35 ± 0.68	0.95 ± 0.68	-8.78 ± 0.67	0.51 ± 0.67
5	2	1	0	6.14 ± 0.66	5.72 ± 0.66	-10.08 ± 0.65	13.79 ± 0.65
6	2	1	1	-5.94 ± 0.67	1.88 ± 0.67	6.05 ± 0.68	3.28 ± 0.68
7	2	2	0	14.47 ± 0.64	4.83 ± 0.64	8.50 ± 0.65	12.55 ± 0.65
8	2	2	1	11.38 ± 0.64	-3.95 ± 0.64	7.12 ± 0.64	-8.79 ± 0.64
9	3	0	1	1.98 ± 0.68	1.33 ± 0.68	-0.27 ± 0.67	-0.71 ± 0.67
10	3	1	0	0.60 ± 0.68	-2.53 ± 0.68	-0.24 ± 0.67	-0.03 ± 0.67
11	3	1	1	-1.58 ± 0.67	-0.43 ± 0.67	-0.32 ± 0.67	2.66 ± 0.67
12	3	2	0	1.25 ± 0.66	-3.76 ± 0.66	8.49 ± 0.65	6.04 ± 0.65
13	3	2	1	4.35 ± 0.66	2.42 ± 0.66	5.95 ± 0.66	-5.60 ± 0.66
14	3	3	0	-0.75 ± 0.62	2.91 ± 0.62	-0.06 ± 0.64	-1.39 ± 0.64
15	3	3	1	-7.88 ± 0.62	0.81 ± 0.62	-4.51 ± 0.63	1.38 ± 0.63
16	4	0	1	3.20 ± 0.67	2.51 ± 0.67	-1.65 ± 0.67	-0.19 ± 0.67
17	4	1	0	-0.45 ± 0.67	-2.95 ± 0.67	0.27 ± 0.64	0.63 ± 0.64
18	4	1	1	-1.79 ± 0.67	3.67 ± 0.67	0.40 ± 0.67	1.25 ± 0.67
19	4	2	0	4.74 ± 0.66	4.53 ± 0.66	2.63 ± 0.66	2.50 ± 0.66
20	4	2	1	0.77 ± 0.66	4.47 ± 0.66	3.93 ± 0.65	-0.23 ± 0.65
21	4	3	0	-1.71 ± 0.64	-2.86 ± 0.64	0.64 ± 0.63	1.62 ± 0.63
22	4	3	1	0.77 ± 0.64	1.67 ± 0.64	0.76 ± 0.64	-0.79 ± 0.64
23	4	4	0	3.48 ± 0.61	5.64 ± 0.61	-0.37 ± 0.62	-2.21 ± 0.62
24	4	4	1	0.89 ± 0.61	0.36 ± 0.61	-0.07 ± 0.62	-2.60 ± 0.62
25	5	0	1	-1.40 ± 0.52	0.04 ± 0.52	-1.72 ± 0.49	-1.80 ± 0.49
26	5	1	0	-1.06 ± 0.52	-2.15 ± 0.52	0.01 ± 0.49	0.88 ± 0.49
27	5	1	1	1.58 ± 0.52	-1.09 ± 0.52	3.18 ± 0.50	-1.53 ± 0.50
28	5	2	0	-0.12 ± 0.52	-1.31 ± 0.52	5.94 ± 0.49	3.04 ± 0.49
29	5	2	1	2.39 ± 0.52	2.03 ± 0.52	1.75 ± 0.50	-6.73 ± 0.50
30	5	3	0	-2.03 ± 0.52	-1.74 ± 0.52	-0.50 ± 0.50	-1.94 ± 0.50
31	5	3	1	-0.63 ± 0.52	-0.11 ± 0.52	0.64 ± 0.50	-0.42 ± 0.50
32	5	4	0	-2.77 ± 0.52	1.62 ± 0.52	3.19 ± 0.51	-4.26 ± 0.51
33	5	4	1	-0.49 ± 0.53	-1.59 ± 0.53	-1.20 ± 0.51	-0.74 ± 0.51
34	5	5	0	-0.17 ± 0.54	-1.73 ± 0.54	-1.96 ± 0.53	-0.88 ± 0.53
35	5	5	1	1.46 ± 0.54	-5.21 ± 0.54	0.04 ± 0.52	3.72 ± 0.52

Note. The units of measurement are km s^{-1} kpc^{-1}.

Table 5. The main and alternative solutions for the UCAC3 stars of the **northern** Galactic hemisphere

Parameters	Main solution				
	12^m	13^m	14^m	15^m	16^m
$U/\langle r\rangle$	11.12 ± 0.57	9.91 ± 0.64	6.73 ± 0.72	3.45 ± 0.87	3.08 ± 0.94
$V/\langle r\rangle$	19.15 ± 0.57	15.03 ± 0.64	10.78 ± 0.72	9.35 ± 0.87	9.85 ± 0.94
$W/\langle r\rangle$	5.23 ± 0.43	4.18 ± 0.49	2.65 ± 0.55	1.99 ± 0.66	1.81 ± 0.72
Ω_1	24.96 ± 0.44	20.12 ± 0.50	20.44 ± 0.57	19.95 ± 0.68	19.51 ± 0.74
Ω_2	-12.95 ± 0.45	-12.73 ± 0.50	-15.04 ± 0.57	-18.19 ± 0.68	-18.02 ± 0.74
Ω_3	-12.62 ± 0.22	-14.02 ± 0.24	-14.18 ± 0.27	-15.03 ± 0.32	-14.89 ± 0.34
M_{13}^+	-8.85 ± 0.51	-6.71 ± 0.58	-6.86 ± 0.65	-7.28 ± 0.79	-4.76 ± 0.85
M_{23}^+	-20.85 ± 0.51	-11.69 ± 0.58	-8.36 ± 0.65	-5.50 ± 0.79	-6.97 ± 0.85
M_{12}^+	11.43 ± 0.32	8.40 ± 0.36	5.49 ± 0.40	3.61 ± 0.47	5.42 ± 0.51
M_{11}^*	-4.20 ± 0.63	-4.49 ± 0.71	-4.96 ± 0.80	-5.90 ± 0.95	-3.42 ± 1.01
M_{33}^*	-17.95 ± 0.99	-8.21 ± 1.12	-5.41 ± 1.26	-2.77 ± 1.53	-0.04 ± 1.65
	Alternative solution				
$U/\langle r\rangle$	14.72 ± 0.94	16.31 ± 1.06	12.38 ± 1.19	6.21 ± 1.43	3.61 ± 1.55
$V/\langle r\rangle$	17.67 ± 0.94	13.95 ± 1.06	8.53 ± 1.19	5.30 ± 1.44	4.70 ± 1.55
$W/\langle r\rangle$	1.10 ± 1.43	-0.94 ± 1.62	-3.38 ± 1.83	-4.09 ± 2.22	-5.33 ± 2.41
Ω_1	25.94 ± 0.63	20.85 ± 0.72	21.84 ± 0.81	22.38 ± 0.97	22.57 ± 1.05
Ω_2	-10.93 ± 0.63	-9.09 ± 0.72	-11.83 ± 0.81	-16.66 ± 0.97	-17.78 ± 1.05
Ω_3	-14.42 ± 0.97	-16.54 ± 1.09	-22.68 ± 1.23	-31.69 ± 1.49	-42.44 ± 1.62
M_{13}^+	-5.10 ± 0.95	0.00 ± 1.07	-0.94 ± 1.21	-4.39 ± 1.45	-4.22 ± 1.57
M_{23}^+	-22.53 ± 0.95	-12.90 ± 1.07	-10.78 ± 1.21	-9.80 ± 1.45	-12.44 ± 1.57
M_{12}^+	4.79 ± 0.97	-7.63 ± 1.10	-18.08 ± 1.23	-26.29 ± 1.47	-29.10 ± 1.57
M_{11}^*	10.68 ± 1.96	20.31 ± 2.20	42.19 ± 2.46	67.01 ± 2.94	90.81 ± 3.15
M_{33}^*	-19.58 ± 3.37	-7.15 ± 3.81	4.80 ± 4.30	20.23 ± 5.20	31.26 ± 5.64

Note. The units of measurement are km s^{-1} kpc^{-1}.

entire celestial sphere, since M_{32}^+ and M_{32}^- are almost the same in magnitude but different in sign, we obtain almost insignificant estimates of these parameters (Table 7).

We will use the Galactocenric cylindrical coordinate system to interpret this result. Since the Galaxy's rotation velocity and the rate of change of the azimuthal angle are directed oppositely, from Eqs. (13) we obtain

$$M_{32}^- - M_{32}^+ = \frac{\partial V_\theta}{\partial z} = -\frac{\partial V_\odot}{\partial z}, \qquad (31)$$

where $V_\odot$ is the circular velocity of the local reference frame around the Galactic center. This quantity is

Table 6. The main and alternative solutions for the UCAC3 stars of the **southern** Galactic hemisphere

Parameters	Main solution				
	12^m	13^m	14^m	15^m	16^m
$U/\langle r\rangle$	8.08 ± 0.65	6.75 ± 0.64	2.27 ± 0.72	-1.35 ± 0.88	-3.02 ± 0.96
$V/\langle r\rangle$	15.01 ± 0.64	7.54 ± 0.63	2.76 ± 0.70	-1.76 ± 0.86	-2.04 ± 0.93
$W/\langle r\rangle$	5.56 ± 0.48	4.52 ± 0.48	3.45 ± 0.53	2.04 ± 0.65	1.09 ± 0.72
Ω_1	-28.27 ± 0.50	-25.48 ± 0.49	-23.85 ± 0.55	-24.05 ± 0.67	-23.44 ± 0.73
Ω_2	5.16 ± 0.51	4.07 ± 0.50	5.38 ± 0.56	5.22 ± 0.69	4.14 ± 0.76
Ω_3	-11.15 ± 0.25	-14.68 ± 0.25	-17.05 ± 0.27	-19.37 ± 0.33	-19.08 ± 0.36
M_{13}^+	9.08 ± 0.60	5.81 ± 0.58	6.72 ± 0.65	6.27 ± 0.80	6.48 ± 0.88
M_{23}^+	29.39 ± 0.58	29.32 ± 0.57	29.07 ± 0.63	29.11 ± 0.77	26.85 ± 0.84
M_{12}^+	14.06 ± 0.37	10.31 ± 0.36	9.31 ± 0.40	9.38 ± 0.49	11.21 ± 0.53
M_{11}^*	-3.58 ± 0.72	-8.21 ± 0.70	-10.95 ± 0.79	-13.14 ± 0.95	-9.84 ± 1.04
M_{33}^*	17.17 ± 1.12	6.27 ± 1.10	0.67 ± 1.23	-1.32 ± 1.51	1.68 ± 1.66
	Alternative solution				
$U/\langle r\rangle$	6.79 ± 1.05	-3.26 ± 1.03	-12.88 ± 1.16	-20.29 ± 1.41	-22.49 ± 1.53
$V/\langle r\rangle$	14.10 ± 1.09	4.42 ± 1.06	-1.74 ± 1.19	-9.46 ± 1.46	-12.34 ± 1.60
$W/\langle r\rangle$	4.36 ± 1.60	0.36 ± 1.58	0.10 ± 1.77	2.83 ± 2.17	4.51 ± 2.38
Ω_1	-28.92 ± 0.73	-27.38 ± 0.71	-26.52 ± 0.80	-28.56 ± 0.98	-29.46 ± 1.07
Ω_2	5.94 ± 0.72	9.88 ± 0.70	14.17 ± 0.79	16.18 ± 0.96	15.41 ± 1.05
Ω_3	-13.54 ± 1.08	-10.04 ± 1.07	-11.90 ± 1.20	-19.38 ± 1.47	-29.57 ± 1.62
M_{13}^+	10.49 ± 1.06	16.39 ± 1.05	22.71 ± 1.17	26.25 ± 1.43	27.02 ± 1.55
M_{23}^+	30.48 ± 1.10	32.72 ± 1.08	33.92 ± 1.21	37.31 ± 1.48	37.79 ± 1.62
M_{12}^+	15.04 ± 1.11	15.28 ± 1.09	15.78 ± 1.21	16.45 ± 1.47	15.21 ± 1.60
M_{11}^*	-4.82 ± 2.31	-25.63 ± 2.23	-39.85 ± 2.47	-39.35 ± 3.01	-18.47 ± 3.27
M_{33}^*	19.09 ± 3.77	6.75 ± 3.72	-6.41 ± 4.17	-16.26 ± 5.11	-10.33 ± 5.60

Note. The units of measurement are km s^{-1} kpc^{-1}.

identified with the Galaxy's rotation velocity in the solar neighborhood.

Table 8 gives the numerical values for the left-hand sides of (31) that we obtained from different star catalogues. We see from this table that the vertical gradient of the Galaxy's rotation velocity $\partial V_\odot/\partial z$ has different signs in the northern and southern Galactic hemispheres, with the velocity itself decreasing with increasing distance from the principal Galactic plane. It is also important that the magnitudes of the gradi-

Table 7. Ogorodnikov–Milne model parameters determined from the UCAC3 catalogue by the LST over the entire celestial sphere

Parameters	12^m	13^m	14^m	15^m	16^m
$U/\langle r\rangle$	15.07 ± 0.15	12.09 ± 0.15	8.72 ± 0.16	5.51 ± 0.18	4.19 ± 0.19
$V/\langle r\rangle$	34.29 ± 0.16	25.06 ± 0.16	19.03 ± 0.17	14.59 ± 0.19	14.05 ± 0.20
$W/\langle r\rangle$	8.99 ± 0.13	5.57 ± 0.13	3.36 ± 0.14	2.01 ± 0.15	1.75 ± 0.15
Ω_1	-0.18 ± 0.19	0.28 ± 0.19	1.48 ± 0.21	2.48 ± 0.25	3.56 ± 0.26
Ω_2	-4.99 ± 0.19	-5.74 ± 0.19	-6.43 ± 0.22	-7.93 ± 0.25	-9.02 ± 0.27
Ω_3	-9.87 ± 0.13	-11.03 ± 0.13	-12.18 ± 0.13	-14.56 ± 0.15	-16.56 ± 0.15
M_{13}^+	-1.33 ± 0.22	-2.11 ± 0.22	-3.14 ± 0.25	-4.45 ± 0.28	-4.49 ± 0.30
M_{23}^+	2.26 ± 0.22	5.18 ± 0.22	6.26 ± 0.24	6.12 ± 0.28	3.74 ± 0.29
M_{12}^+	14.20 ± 0.18	11.78 ± 0.17	10.27 ± 0.18	10.02 ± 0.19	11.66 ± 0.20
M_{11}^*	-1.77 ± 0.34	-4.03 ± 0.33	-6.08 ± 0.36	-9.24 ± 0.39	-9.74 ± 0.39
M_{33}^*	1.71 ± 0.46	1.87 ± 0.46	1.67 ± 0.50	1.54 ± 0.56	2.32 ± 0.58

Note. The units of measurement are km s^{-1} kpc^{-1}.

Table 8. Estimates of the differences and sums of M_{32}^- and M_{32}^+ for the northern (N) and southern (S) Galactic hemispheres

Catalogue	$(M_{32}^- - M_{32}^+)_N$	$(M_{32}^- - M_{32}^+)_S$	$(M_{32}^- + M_{32}^+)_N$	$(M_{32}^- + M_{32}^+)_S$
UCAC3, $12-13^m$	38.8 ± 0.5	-56.2 ± 0.5	-13.1 ± 0.7	2.5 ± 0.5
UCAC3, $14-16^m$	26.9 ± 0.6	-52.1 ± 0.6	-2.7 ± 0.9	4.6 ± 0.6
Tycho-2 R, $10-12^m$	50.5 ± 1.2	-47.8 ± 1.0	-3.9 ± 1.2	4.3 ± 1.0
HIP.R, 250–500 pc	22.0 ± 4.1	-18.2 ± 4.0	-5.7 ± 4.1	2.5 ± 4.0

The units of measurement are km s^{-1} kpc^{-1}.

ent are approximately identical for the stars to 13^m from all three catalogues. Only the subset of faint (14^m-17^m) UCAC3 stars constitutes an exception. Averaging these results over both hemispheres, it can be said that the magnitude of the vertical gradient of the Galaxy's rotation velocity for the stars to 13^m is determined very reliably and lies within the range

$$(20.1 \pm 2.9) < \left|\frac{\partial V_\odot}{\partial z}\right| < (49.2 \pm 0.8)\ \text{km s}^{-1}\ \text{kpc}^{-1}. \quad (32)$$

Note that the lower limit was obtained from the Hipparcos red giants, while the upper one is almost the same for the Tycho-2 and UCAC3 catalogues.

There is extensive literature devoted to determining the vertical gradient of the Galaxy's rotation velocity (Majewski 1993; Girard 2006). However, it should be noted that the first studies of the Galaxy's rotational retardation were carried out by various indirect methods. For example, Hanson (1989) proceeded from the increase in the component V_y of solar motion relative to stars with their distances from the Galactic plane and established that the gradient was 30 km s^{-1} kpc^{-1} for the Galactic thick disk (1–4 kpc). Based on the overall Galactic potential model, Girard (2006) offered a dynamical explanation for the negative linear gradient of rotation velocity with distance from the Galactic plane. Makarov and Murphy (2007) hypothesized that this gradient also exists in the thin disk (200–300 pc). They found the gradient from Hipparcos data to be 20 km s^{-1} kpc^{-1}, which is completely confirmed by our results. In contrast to the listed methods, our approach can be classified as a direct method, because we detected an alternation of the vertical velocity gradient by analyzing the parameters of the Ogorodnikov–Milne model applied separately to the northern and southern

Table 9. Estimates of the differences and sums of M_{13}^- and M_{13}^+ for the northern (N) and southern (S) Galactic hemispheres

Catalogue	$(M_{13}^- - M_{13}^+)_{\rm N}$	$(M_{13}^- - M_{13}^+)_{\rm S}$	$(M_{13}^- + M_{13}^+)_{\rm N}$	$(M_{13}^- + M_{13}^+)_{\rm S}$
UCAC3, $11-13^m$	-4.3 ± 0.5	-4.6 ± 0.5	-23.3 ± 0.5	14.4 ± 0.5
UCAC3, $14-17^m$	-11.2 ± 0.5	-2.3 ± 0.5	-22.2 ± 0.5	10.8 ± 0.5
Tycho-2 R, $10-12^m$	0.9 ± 1.2	-2.2 ± 1.0	-20.4 ± 1.2	15.0 ± 1.0
HIP.R, 250–500 pc	0.2 ± 4.2	2.1 ± 4.1	-12.4 ± 4.2	2.7 ± 4.1

Note. The units of measurement are km s^{-1} kpc^{-1}.

Galactic hemispheres, where this gradient retains its sign.

From Eqs. (13) we obtain

$$M_{32}^- + M_{32}^+ = -\frac{1}{R}\frac{\partial V_z}{\partial \theta}. \quad (33)$$

Miyamoto and Zi Zhu (1998) and Zi Zhu (2000) associated this quantity with a kinematic manifestation of the local Galactic warp. From the proper motions of Hipparcos $O-B5$ stars, these authors determined

$$-\frac{1}{R}\frac{\partial V_z}{\partial \theta} = 3.79 \pm 1.05 \text{ km s}^{-1} \text{ kpc}^{-1}. \quad (34)$$

This value is in good agreement with that derived previously (Miyamoto et al. 1993) from the ACRS catalogue (Corbin and Urban 1991)

At the same time, while investigating the Hipparcos proper motions, Mignard (2000) found no evidence of the Galactic warp. As follows from Table 8, our calculations based on the Hipparcos catalogue confirm Mignard's conclusion, because they give statistically unreliable values for the sought-for quantity. Nevertheless, our estimates of this quantity based on the UCAC3 and Tycho-2 catalogues turned out to be statistically reliable. At the same time, they also change their sign when passing from the northern hemisphere to the southern one, showing good agreement with one another in each hemisphere for all samples from these catalogues (Table 8). Note that the value (34) is confirmed only in the southern Galactic hemisphere; its sign is opposite in the northern hemisphere. For this reason, it is unlikely that the behavior of the sum of $M_{32}^- + M_{32}^+$ is a consequence of the Galactic warp.

Analysis of the Parameters M_{13}^- and M_{13}^+. The Vertical Gradient of Expansion Velocity for the Stellar System

As follows from Eqs. (12), these parameters in the Galactocentric coordinate system allow the following quantities to be determined:

$$M_{13}^- - M_{13}^+ = \frac{\partial V_z}{\partial R}, \quad (35)$$

$$M_{13}^- + M_{13}^+ = -\frac{\partial V_R}{\partial z}. \quad (36)$$

The first relation defines the radial gradient of the vertical velocity field component, while the second relation defines the vertical gradient of the expansion velocity of the stellar system. Table 9 shows the numerical values of these quantities that we derived from different catalogues. We see that the results obtained from the Tycho-2 and Hipparcos catalogues for the first of these two gradients turned out to be statistically insignificant, while the UCAC3 catalogue gives statistically reliable negative values for the gradient $\partial V_z/\partial R$, indicating that the vertical velocity component decreases with increasing Galactocentric distance. Interestingly, $M_{13}^- - M_{13}^+ = -3.9 \pm 0.2$ km s^{-1} kpc^{-1} obtained for the entire UCAC3 sphere (Table 7) agrees well with the solutions for the hemispheres.

In addition, we have a very interesting result for the vertical gradient of the expansion velocity of the stellar system $\partial V_R/\partial z$. We see excellent agreement for the UCAC3 and Tycho-2 catalogues and the results for the Hipparcos catalogue consistent with them. These results give positive and negative values for our gradient in the northern and southern hemispheres, respectively. For the solution for the entire sphere, the mean value of (36) turned out to be $M_{13}^- + M_{13}^+ = -9.7 \pm 0.2$ km s^{-1} kpc^{-1}, which is equal to the sum of the corresponding values obtained for different hemispheres. This suggests that the expansion velocity V_R increases with distance from the Galactic plane. This conclusion needs to be confirmed by the dynamics of stellar systems.

Solar Motion Components

Analysis of the parameters M_{32}^- and M_{32}^+ when they are determined for the northern and southern hemispheres separately shows a stable picture: these parameters are approximately identical in magnitude

but change their signs when passing from one hemisphere to the other. The parameters M_{13}^- and M_{31}^+ behave similarly.

It can be shown that such a behavior of these parameters affects the determination of U and V (the solar motion components along the x and y axes). For this purpose, let us produce an artificial catalogue of stellar proper motions on the entire sphere in accordance with the formulas

$$(\mu_l)\cos b = -M_{32}^- \sin b\cos l + M_{23}^+ \sin b\cos l - M_{13}^- \sin b\sin l - M_{13}^+ \sin b\sin l, \quad (37)$$

$$(\mu_b) = M_{32}^- \sin l + M_{23}^+ \cos 2b\cos l - M_{13}^- \cos l + M_{13}^+ \cos 2b\cos l \quad (38)$$

and take here the values of

$$M_{13}^- = \mp 10, \quad M_{13}^+ = \mp 10 \text{ km s}^{-1} \text{ kpc}^{-1},$$
$$M_{32}^- = \pm 25, \quad M_{32}^+ = \mp 25 \text{ km s}^{-1} \text{ kpc}^{-1}$$

typical of the Tycho-2 catalogue, where the upper and lower signs refer to the northern and southern hemispheres, respectively. Decomposing these proper motions into a system of VSHs determined on the entire sphere using the procedure described previously (Vityazev and Tsvetkov 2009), we will obtain

$$s_{110} = -81.4, \quad s_{310} = -29.7, \quad t_{211} = 35.0,$$
$$s_{111} = -32.6, \quad s_{311} = -8.3, \quad t_{210} = -14.0.$$

Let us dwell on the situation described by the coefficients s_{110} and s_{111}, because these harmonics determine the solar motion components along the y and x axes, respectively (Vityazev and Tsvetkov 2009). Using the VSH components $S_{110}(l,b)$ and $S_{111}(l,b)$ in explicit form, let us write Eqs. (8) and (9) by retaining only the terms containing the solar motion components U, V and the VSH components $S_{110}(l,b)$, $S_{111}(l,b)$:

$$x/r\sin l - y/r\cos l = U/r\sin l - a_x\sin l - V/r\cos l + a_y\cos l, \quad (39)$$

$$x/r\cos l\sin b + y/r\sin l\sin b = U/r\cos l\sin b - a_x\cos l\sin b + V/r\sin l\sin b - a_y\sin l\sin b, \quad (40)$$

where we use the notation $a_x = 0.345$; $s_{111} = -11.2$; $a_y = 0.345$; $s_{110} = -28.1$.

Let us find the combined solution of these equations by the least-squares technique. If the distances to the stars are unknown, then the solution is performed for the quantities $\langle x/r\rangle$ and $\langle y/r\rangle$, instead of which we actually obtain

$$\langle x/r\rangle = \langle U/r\rangle - a_x, \quad \langle y/r\rangle = \langle V/r\rangle - a_y. \quad (41)$$

If the individual distances to the stars are known, then they are taken into account in the solution. In the idealized case where all stars are at the same distance r from us, as the solution we obtain not the components U and V themselves but the quantities

$$x = U - a_x r, \quad y = V - a_y r. \quad (42)$$

Our numerical experiments showed that Eqs. (41) and (42) are a good approximation for the situations where the stars are located in spherical layers up to 300 pc in thickness. In these cases, r in Eq. (42) should be replaced by the mean distance to the stars $\langle r\rangle$.

If the parameter a_y is determined by the vertical gradient of the Galaxy's rotational velocity, then its value is negative and, as follows from Eq. (42), the quantity y taken as the solar motion component V increases linearly at the rate

$$\frac{dy}{dr} = -a_y = 28.1 \text{ km s}^{-1} \text{ kpc}^{-1}$$

with increasing mean distance to the stars (we give the numerical estimates from the Tycho-2 catalogue). This fact was probably first established by Hanson (1989), who estimated the gradient to be 30 km s^{-1} kpc^{-1}. It was also pointed out by Makarov and Murphy (2007) and was explained by them by one of several factors, including the influence of the vertical gradient of the Galaxy's rotation velocity. Our result removes the uncertainty in choosing these factors and shows that the acceleration of solar motion with respect to distant stars is further evidence for the Galaxy's rotational retardation with increasing z coordinate. Note that statistically significant coefficients s_{310} and t_{211}, which do not enter into the Ogorodnikov–Milne model, were first found by Vityazev and Shuksto (2003) when performing a kinematic analysis of the proper motions of Hipparcos stars distributed over the entire sphere. Subsequently, this result was confirmed by Makarov and Murphy (2007) as well as by Vityazev and Tsvetkov (2009). We now see that in the case of analysis over the entire sphere, the vertical gradient of the Galaxy's rotation velocity, on the one hand, gives rise to the "beyond-model" harmonics s_{110}, s_{310}, and t_{211} and, on the other hand, produces an acceleration of the solar motion along the y axis with increasing distance to the stars.

Obviously, there is a similar effect in the solar motion along the x axis due to the existence of a vertical expansion velocity gradient $\partial V_R/\partial z$. This gradient gives rise to a different series of harmonics when performing a kinematic analysis of the stars

Table 10. Estimates of the differences and sums of M_{21}^- and M_{12}^+ for the northern (N) and southern (S) Galactic hemispheres

Catalogue	$(M_{21}^- - M_{12}^+)_\mathrm{N}$	$(M_{21}^- - M_{12}^+)_\mathrm{S}$	$(M_{21}^- + M_{12}^+)_\mathrm{N}$	$(M_{21}^- + M_{12}^+)_\mathrm{S}$
UCAC3, 11^m–13^m	-23.7 ± 0.4	-25.2 ± 0.6	-21.6 ± 0.5	-3.2 ± 0.4
UCAC3, 14^m–17^m	-19.8 ± 0.7	-28.4 ± 0.7	-21.7 ± 0.9	-11.7 ± 0.7
Tycho-2 R, 10^m–12^m	-24.6 ± 0.7	-28.4 ± 0.6	-4.9 ± 0.7	9.0 ± 0.6
HIP.R, 250–500 pc	-27.3 ± 2.4	-29.4 ± 2.3	1.0 ± 2.3	1.9 ± 2.3

Note. The units of measurement are km s^{-1} kpc^{-1}.

over the entire sphere. For example, from the Tycho-2 catalogue we have

$$s_{111} = -60.7 \pm 0.8, \quad s_{311} = -8.4 \pm 0.8,$$
$$t_{210} = -13.4 \pm 0.8,$$

while from the samples of UCAC3 14^m–15^m and 15^m–16^m stars we obtained

$$s_{111} = -41.3 \pm 0.4, \quad s_{310} = -2.9 \pm 0.4,$$
$$t_{210} = -16.9 \pm 0.4,$$

$$s_{111} = -33.7 \pm 0.5, \quad s_{311} = -2.0 \pm 0.5,$$
$$t_{210} = -20.4 \pm 0.4.$$

Consequently, if a_x is determined by the behavior of M_{13}^- and M_{31}^+, then its value is negative and, as follows from Eq. (42), the quantity x taken as the solar motion component along the x axis increases linearly at the rate

$$\frac{dx}{dr} = -a_x = 11.2 \text{ km s}^{-1} \text{ kpc}^{-1}$$

(we give the numerical estimate from the Tycho-2 catalogue). This effect is not very large; that is the possible reason why it is not pointed out in the literature.

Analysis of the Parameters M_{21}^- and M_{12}^+. Galactic Rotation

In what follows, we will dwell on the results of our analysis, which turned out to be almost identical for both Galactic hemispheres. This primarily applies to the Oort parameters A and B and to all of the Galactic rotation characteristics via which they are defined. Indeed, from Eqs. (11) we obtain

$$M_{21}^- - M_{12}^+ = \frac{V_\theta}{R} + \frac{1}{R}\frac{\partial V_R}{\partial \theta}. \quad (43)$$

Let us set here

$$\partial V_R / \partial \theta = 0. \quad (44)$$

When this condition is met, we can introduce the Oort parameters A and B:

$$A = M_{12}^+, B = M_{21}^-. \quad (45)$$

Since the Galactic rotation is opposite to the direction in which the azimuthal angle is measured, from Eq. (46) we obtain

$$V_\odot = -R_\odot (M_{21}^- - M_{12}^+) \quad (46)$$

for the circular velocity of the local reference frame $V_\odot$ (the Galaxy's rotational velocity in the solar neighborhood), where $R_\odot$ denotes the Galactocentric distance of the Sun.

In accordance with the epicyclic theory (Binney and Tremaine 1987; Mignard 2000), the ratio of the epicyclic frequency k_0 to the angular velocity of Galactic rotation Ω_0 in the solar neighborhood can be estimated:

$$\frac{k_0}{\Omega_0} = 2\sqrt{\frac{-B}{A-B}}. \quad (47)$$

In addition, it follows from (11) that the slope of the Galactic rotation curve or the radial gradient of the Galaxy's rotation velocity can be determined using the expression

$$M_{21}^- + M_{12}^+ = -\frac{\partial V_\odot}{\partial R}. \quad (48)$$

The numerical estimates of the differences and sums of M_{21}^- and M_{12}^+ that we obtained from various samples from the UCAC3, Tycho-2, and Hipparcos catalogues are shown in Table 10.

We see from Table 10 that the values of $(M_{21}^- - M_{12}^+)$ in the northern and southern hemispheres do not differ greatly for the stars to 12^m from different catalogues. This allows us to obtain various Galactic rotation characteristics by averaging the derived values of M_{21}^- and M_{12}^+. The results of this averaging are presented in Table 11. Note that they are in good agreement with the results obtained through a kinematic analysis of the stellar proper motions over the entire celestial sphere (Binney and Tremaine 1987;

Table 11. Differences of M_{21}^- and M_{12}^+ averaged over the northern and southern Galactic hemispheres, estimates of the Galaxy's rotational velocity in km s^{-1} in the solar neighborhood (for $R_\odot = 7.5$ kpc), and estimates of the Galactic rotation period in Myr

Catalogue	$M_{21}^- - M_{12}^+$	$V_\odot$	Period	k_0/Ω_0
UCAC3, 11^m–13^m	-24.5 ± 0.7	183.8 ± 4.5	250.6 ± 6.1	1.42 ± 0.01
Tycho-2 R, 10^m–12^m	-26.5 ± 0.7	198.8 ± 5.3	231.0 ± 6.1	1.36 ± 0.01
HIP.R, 250–500 pc	-28.4 ± 2.4	213.0 ± 18.8	216.2 ± 18.2	1.38 ± 0.04

Note. The last column gives k_0/Ω_0, the ratio of the epicyclic frequency to the angular velocity of Galactic rotation in the solar neighborhood.

Table 12. Estimates of the parameters M_{11}^* and M_{12}^+ in km s^{-1} kpc^{-1} and the phase angle ϕ in degrees from different samples of stars from different catalogues

Parameters	UCAC3	Tycho-2 W	Tycho-2 Y	Tycho-2 R	HIP.B	HIP.R
M_{11}^*	-5.3 ± 0.5	-6.7 ± 0.3	-8.0 ± 1.2	-3.7 ± 0.7	-9.4 ± 1.7	-8.4 ± 2.0
M_{12}^+	12.1 ± 0.2	13.3 ± 0.2	14.3 ± 0.6	14.0 ± 0.4	12.5 ± 0.9	14.6 ± 1.0
ϕ	6.2 ± 0.6	7.1 ± 0.3	7.8 ± 1.26	3.8 ± 0.7	10.4 ± 1.9	8.0 ± 1.9

Note. The UCAC3 and Tycho-2 stars were taken from the ranges 11^m–17^m and 6^m–14^m, respectively; the sample of Hipparcos stars corresponds to the range of distances from 100 to 1000 pc. The symbols B, W, Y, and R denote the blue, white, yellow, and red stars, respectively.

Mignard 2000; and others). As regards the slope of the Galactic rotation curve, our estimates for the stars to 13^m from the Hipparcos and Tycho-2 catalogues are very contradictory and do not allow this quantity to be estimated reliably. For the UCAC3 catalogue the estimates are found to be statistically reliable. However, although they retain their sign in both hemispheres, they differ greatly in absolute value. The differences of M_{21}^- and M_{12}^+ for the samples of faint (14^m–17^m) stars from the UCAC3 catalogue also exhibit the same behavior.

Diagonal Elements of the Velocity Field Deformation Tensor

As has already been said above, when the stellar proper motions are analyzed, only two of the three components M_{11}^+, M_{22}^+, M_{33}^+ can be determined: $M_{11}^* = M_{11}^+ - M_{22}^+$ and $M_{33}^* = M_{33}^+ - M_{22}^+$. Our values of the parameter M_{33}^* do not allow them to be used to obtain trustworthy physical information, because they are either insignificant (according to the "three sigma" criterion) or contradictory from comparison of the main and alternative solutions. The determination of M_{11}^* gives a completely different picture. Table 12 lists the values of this parameter that we derived from different samples of stars from different catalogues. It should be said that the values of this quantity obtained for different hemispheres are essentially the same. Therefore, we provide the values derived for the solution over the entire sphere. The values of M_{11}^* that we calculated from different catalogues are in good agreement with the results by Makarov and Murphy (2007) obtained from the sample of stars with distances $r > 100$ pc from the Hipparcos catalogue (-9.44 ± 2.38 km s^{-1} kpc^{-1}).

Note that Mignard (2000) showed that

$$\phi = -\frac{1}{2}\arctan\left(\frac{M_{11}^*}{2M_{12}^+}\right) \qquad (49)$$

determines the angle of rotation of the Galactic coordinate system triad around the z axis, which is equivalent to the introduction of a new origin for the Galactic longitudes. This rotation ensures that the conditions $M_{11}^+ = 0$ and $M_{22}^+ = 0$ are met. Interestingly, the values of this angle obtained by Mignard from different samples of Hipparcos stars lie within the range from $0.2^\circ \pm 2.5^\circ$ to $16.4^\circ \pm 4.0^\circ$. Our values obtained from different catalogues (Table 12) agree well with these values but within a smaller range. All of this suggests that the orientation of the rectangular Galactic coordinate system in space must be determined by taking into account not only the geometrical factors but also the dynamical ones.

CONCLUSIONS

A kinematic analysis of the proper motions of stars separately in the northern and southern Galactic hemispheres may be considered to be our main result. For this purpose, we used our method of zonal vector spherical harmonics with the properties of completeness and orthogonality in each of these hemispheres. Our method has the following advantages over the direct estimation of kinematic model parameters by the least-squares technique: (1) the ZVSH method reveals any systematic components of the stellar velocity field irrespective of the kinematic model; (2) the ZVSH method allows the parameters of any kinematic model to be determined; (3) in contrast to the standard procedure for estimating the kinematic model parameters, the ZVSH method allows at least two estimates of the sought-for parameters (the main and alternative ones) to be obtained. Their comparison makes it possible to judge whether the model is consistent with the observational data.

All these properties were confirmed by our numerical experiments following which we applied our method to analyze the proper motions of stars from the Hipparcos, Tycho-2, and UCAC3 catalogues. The results obtained in the local coordinate system comoving with the Sun were transformed to the Galactocentric cylindrical coordinate system relative to which the velocity field components and their gradients were obtained. Analysis of the components M_{12}^{+} and M_{21}^{-} of the displacement matrix M in Eq. (4) revealed no distinct differences in the Oort parameters and the Galaxy's rotational velocity estimates found for different hemispheres. In contrast, the components with indices $(1,3)$ and $(2,3)$ allowed the effects of the Galaxy's rotational retardation and the effect of an increase in the expansion velocity of the stellar system as the stars recede from the principal plane to be detected. The numerical estimates of the vertical gradient of the Galaxy's rotation velocity that we obtained by a direct method are in good agreement with the results of determining this gradient found by other authors by indirect methods. In turn, both these gradients give rise to an apparent acceleration of the solar motion along the x and y axes of the rectangular Galactic coordinate system.

REFERENCES

1. G. Arfken, *Mathematical Methods for Physicists* (Academic, New York, 2000; Atomizdat, Moscow, 1970), p. 493.
2. J. Binney and S. Tremaine, *Galactic Dynamics* (Princeton Univ. Press, Princeton, 1994).
3. V. V. Bobylev , G. A. Goncharov, and A. T. Baikova, Astron. Rep. **50**, 733 (2006).
4. V. V. Bobylev and M. Yu. Khovritchev, Mon. Not. R. Astron. Soc. **417**, 1952 (2011).
5. L. R. Branham, Jr., Astrophys. J. **570**, 190 (2002).
6. P. Brosche, Veröff, des Astron. Rechen-Inst. Heidelberg N **17**, 1 (1966).
7. T. E. Corbin and S. E. Urban, ACRS, USNO (1991).
8. A. L. Coryn and Bailer-Jones, Mem. S. A. It. **77**, 1c SAIt (2004).
9. R. Drimmel, R. L. Smart, M. G. Lattanzi, et al., Astron. Astrophys. **354**, 67 (2000).
10. F. K. Edmondson, Mon. Not. R. Astron. Soc. **97**, 473 (1937).
11. T. M. Girard, Astron. J. **132**, 1768 (2006).
12. K. M. Gorski, E. Hivon, A. J. Banday, et al., Astrophys. J. **622**, 759 (2005).
13. R. Hanson, Astron. J. **94**, 409 (1989).
14. E. Hog, C. Fabricius, V. V. Makarov, et al., Astron. Astrophys. **355**, L27 (2000).
15. S. R. Majewski, Ann. Rev. Astron. Astrophys. **31**, 575 (1993).
16. V. V. Makarov and D. W. Murphy, Astron. J. **134**, 367 (2007).
17. F. Mignard, Astron. Astrophys. **354**, 522 (2000).
18. F. Mignard and B. Morando, *Journees 90. Systemes de Reference Spatio-Temporels* (Paris, 1990), pp. 151–158.
19. M. Miyamoto and Zi Zhu, Astron. J. **115**, 1483 (1993).
20. M. Miyamoto, M. Soma, and M. Yokoshima, Astron. J. **105**, 2138 (1993).
21. D. G. Monet, S. E. Levin, B. Canzian, et al., Astron. J. **125**, 984 (2003).
22. B. A. du Mont, Astron. Astrophys. **61**, 127 (1977).
23. K. F. Ogorodnikov, *Dynamics of Stellar Systems* (Fizmatgiz, Moscow, 1965) [in Russian].
24. M. A. C. Perriman et al., *The Hipparcos and TYycho Catalogues*, ESA SP-1200 (1997), Vols. 1–17.
25. S. Roeser, M. Demleitner, and E. Schilbach, Astron. J. **139**, 2440 (2010).
26. M. F. Skrutskie, R. M. Cutri, R. Stiening, et al., Astron. J. **131**, 1163 (2006).
27. V. V. Vityazev and A. S. Tsvetkov, Vestn. Leningr. Univ., Ser. 1, No. 2, 73 (1989).
28. V. Vityazev and A. Shuksto, ASP Conf. Ser. **316**, 230 (2004).
29. V. V. Vityazev and A. K. Shuksto, Vestn. SPb. Univ., Ser. 1, No. 1, 116 (2005).
30. V. V. Vityazev and A. S. Tsvetkov, Astron. Lett. **35**, 100 (2009).
31. V. V. Vityazev and A. S. Tsvetkov, Astron. Lett. **37**, 874 (2011).
32. N. Zacharias et al., CDS Strasbourg, I/315 (2009).
33. Zi Zhu, Publ. Astron. Soc. Jpn. **52**, 1133 (2000).

Translated by V. Astakhov